Probing Dense Medium by Dijets

Rudolph C. Hwa
Institute of Theoretical Science and Department of Physics
University of Oregon, Eugene, OR 97403-5203, USA

Abstract

A brief summary is given of the study of the correlation between trigger and associated particles in jets produced on near and away sides in heavy-ion collisions. Using the recombination model to relate the observed particles to the parton momenta for hadron p_T in the intermediate range ($2 < p_T < 6$ GeV/c), it is possible to learn about the average fractional energy losses of the partons on both sides, as functions of the hadron momenta. Medium thicknesses experienced by the back-to-back partons are allowed to vary for every centrality, for which a reliable description of the dynamical path length is found. Because of trigger and anti-trigger biases, the medium interior is not well probed. Symmetric dijets turn out to be dominated by tangential jets. Averaging over various variables, such as the azimuthal angles, reduces the effectiveness of jet tomography.

PACS numbers: 25.75.-q, 25.75.Gz, 24.85.+p

1 Introduction

In this general talk on jet-medium interaction in heavy-ion collisions, I shall try to avoid details and attempt to convey central ideas and main results. The buzz words these days in the RHIC community, theoretical as well as experimental, are ridges and double-hump structures in dihadron correlation. They are the response of a dense medium to the passage of a hard parton through it. I will not talk about them in order to have enough time to discuss the reverse problem, i.e., the effect of the medium on the hard parton. The question is: what can we learn about the medium by studying jets, especially back-to-back dijets? Jet tomography is not as it was expected to be. Because of the necessity to average over many events that have different orientations of the probed medium, what one can see is like overlaying many chest X-ray films of subjects of different sizes and varying standing positions without adequate spatial resolution. To understand that there is such a mess is the first step toward finding a way to disentangle the mess.

Dijets that are back-to-back are the simplest correlation experiment to understand theoretically, since they involve two hard partons moving in opposite directions through the medium. Restricting the dijets to only the transverse plane further simplifies the problem by circumventing the complications of longitudinal expansion. A hadron in each jet is easier to detect than the whole jet on each side. The theoretical work required to determine the probability of finding a hadron of certain momentum fraction within a jet is somewhat more complicated, but we have experience with studying single-particle distribution in a framework of hadronization that reproduces the data very well. Fig. 1 shows the inclusive spectra of π^0 over a wide range of p_T and for 9 bins of centrality [1]. The lines are calculated in the recombination model that includes all three components of $TT + TS + SS$ recombination [2, 3]. Using that framework as a basis to relate hadrons to the partons at the surface, we therefore can focus on the momentum degradation of hard partons from the point of creation to the points of emergence from the medium, and describe the medium effect in terms of hadron momenta that are measurable.

In order to interpret properly the results on dihadron correlation on opposite sides, it is necessary to know first such correlation within the same jet. By comparing the same-side and away-side correlations, we are led to the study of symmetric jets that reveal some properties from which some general conclusions can be drawn.

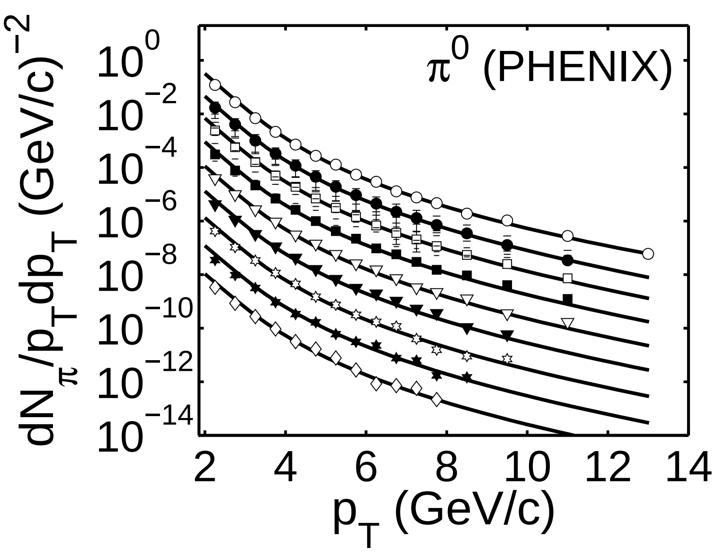

Figure 1: Inclusive distribution of π^0 for all centralities ranging from 0-10% (top) to 80-92% (bottom) in 10% steps, each displaced by a factor of 0.2. The data are from Ref. [1]. The lines are calculated in the recombination model [2, 3].

2 Formalism

The basis of our calculation is recombination [2, 3], which we describe very briefly here. By simplifying the hadronization problem to 1-dimension along the direction of a detected pion in the transverse plane with all relevant partons being collinear, we can write for the invariant distribution

$$p^0 \frac{dN_\pi}{dp} = \int \frac{dq_1}{q_1} \frac{dq_2}{q_2} F_{q\bar{q}}(q_1, q_2) R_\pi(q_1, q_2, p), \tag{1}$$

where R_π is the recombination function

$$R_\pi(q_1, q_2, p) = \frac{q_1 q_2}{p^2} \delta \left(\frac{q_1}{p} + \frac{q_2}{p} - 1 \right), \tag{2}$$

and $F_{q\bar{q}}$ is the quark-antiquark distribution that contains what we look for about jet-medium interaction. It can be separated into three components: $F_{q\bar{q}} = TT + TS + SS$. The thermal parton distribution T is extracted from low-p_T pion spectra. It is the shower parton distribution (SPD) S that carries the information about the medium effect on hard partons. If $F_i(q)$ denotes the parton distribution at the surface before hadronization, then the SPD is

$$S(q_1) = \int \frac{dq}{q} F_i(q) S_i^j(q_1/q), \tag{3}$$

where $S_i^j(z)$ is the probability of finding a shower parton j of momentum fraction z in a hard parton i and is known [4]. The crux of the problem therefore lies in $F_i(q)$.

The production of a hard parton of momentum k at the point of creation has a distribution $f_i(k)$ that has been parameterized [5]. How $f_i(k)$ is transformed into $F_i(q)$, as the parton loses energy from k to q while traversing the medium of thickness L, is described by

$$F_i(q) = \int_0^L \frac{dt}{L} \int_{k_0}^{\infty} dk k f_i(k) G(q, k, t), \tag{4}$$

where $G(q, k, t)$ is the momentum degradation factor, and k_0 is a lower limit set at 3 GeV in calculation. It is argued in [3] that a reasonable expression for the degradation factor is

$$G(q, k, t) = q \delta(q - k e^{-\beta t}), \tag{5}$$

where k is damped exponentially in path length t with β being the unknown coefficient of degradation. Putting (5) in (4) yields

$$F_i(q) = \frac{1}{\beta L} \int_q^{q e^{\beta L}} dk k f_i(k), \tag{6}$$

which relates $f_i(k)$ before degradation to $F_i(q)$ at the medium surface. Note that the medium effect enters that relationship through the dimensionless quantity βL for a fixed thickness L. βL is an average of the dynamical path length (DPL), which for central Au+Au collisions at 200 GeV turns out to be $\beta L = 2.9$, an input used to reproduce the π^0 data at 0-10% centrality, shown by the top curve in Fig. 1.

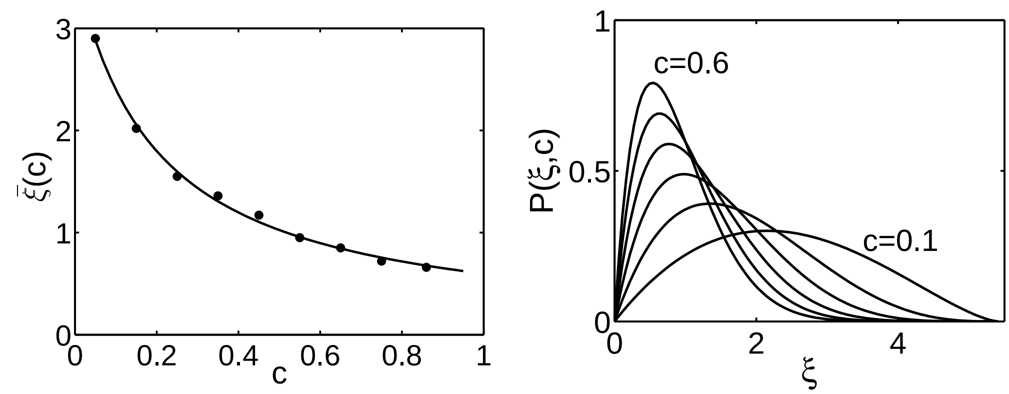

Figure 2: (a) The dots are the values of $\beta L(c)$ used to fit the inclusive distributions in Fig. 1. The solid line is the average $\bar{\xi}(c)$ from the ξ distribution $P(\xi, c)$ given in Eq. (7). (b) The distribution of the dynamical path length ξ for six values of centrality c in steps of 0.1.

For any centrality the actual DPL can vary widely from the average, since the parton trajectory can be as short as 0, or as long as the diameter of the nucleus for head-on collision. Let c denote centrality in %, e.g., c = 0.5 for 50% mid-central collision. Let the actual DPL be denoted by ξ so that for each c the average is $\beta L = \bar{\xi}(c)$. The nine bins of c in Fig. 1 from $c = 0.05$ to $c = 0.86$ provide nine values of $\bar{\xi}(c)$, when Eqs. (1) and (6) are used to fit all the data points in Fig. 1 with βL being the only free parameter adjusted for each c. The resultant $\bar{\xi}(c)$ are shown by the nine points in Fig. 2(a). Those points can be described in a unified way when we use a two-parameter formula

$$P(\xi, c) = N\xi(\xi_0 - \xi)^{\alpha c} \tag{7}$$

for the probability for the DPL to be ξ at c, N being the normalization factor. Based on (7) the average $\bar{\xi}(c)$ can be calculated and can fit all nine points in Fig. 2(a) very well when the parameters ξ_0 and α are set at

$$\xi_0 = 5.42, \qquad \alpha = 15.2, \tag{8}$$

as shown by the solid line in Fig. 2(a). Thus over 100 data points in Fig. 1 are now summarized by the two parameters in (8). The probability distributions (7) are displayed in Fig. 2(b) for six values of c. Since $\beta L(c)$ cannot be derived from first principles for $2 < p_T < 12$ GeV/c, let alone $P(\xi, c)$, we regard (7) and (8), obtained in [3], as being totally satisfactory for the description of DPL at any centrality.

3 Dihadron Correlations

The dihadron correlations that we consider are of two types: both hadrons are on the same side or the two are on opposite sides. Using a trigger as the reference, the associated particle in the former case is on the *near* side, while that in the latter case is on the *away* side. The momenta of the three particles are, respectively, denoted by p_t, p_a and p_b. They are measurable, but the partons that produce them are not. To clarify and exhibit the various momentum variables in the transverse plane, we sketch them in Fig. 3, where k and q are partons on the near side and k' and q' are partons on the away side. The magnitudes of k and k' at the point of hard scattering are equal if the initial transverse momenta of the colliding partons are neglected. However, their averages $\langle k \rangle$ and $\langle k' \rangle$ need not be the same, depending on what observables among p_t, p_a and p_b are held fixed.

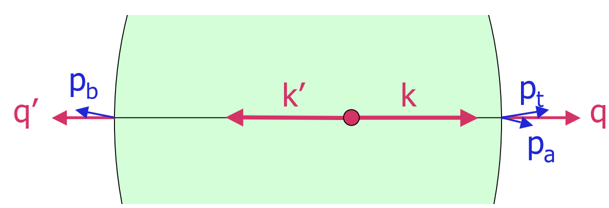

Figure 3: (Color online) A sketch of momentum vectors of partons (in red) and hadrons (in blue) with near side being on the right and away side on the left.

Dihadron distribution on the same side, $dN/p_t p_a dp_t dp_a$, involves an integration over q of the parton distribution $F_i(q)$ discussed earlier in (6). But the dihadron distribution on opposite sides, $dN/p_t p_b dp_t dp_b$, involves the diparton distribution $F_i'(q, q')$, where to reduce complexity it is assumed that the recoiling parton i' is $\bar{i}$ if it is a quark, and is i if it is a gluon, and that the two hadrons are identical pions. Using the same degradation factor $G(q', k', L - t)$ for the away side as for the near side, we have

$$F_i'(q, q') = \frac{1}{\bar{\xi}(c)} \int_q^{qe^{\bar{\xi}(c)}} dk k f_i(k) q q' \delta(q q' - k^2 e^{-\bar{\xi}(c)}). \tag{9}$$

The two-pion distribution is then

$$\frac{dN_{\pi\pi}}{p_t p_b dp_t dp_b} = \frac{1}{(p_t p_b)^2}\sum_i \int \frac{dq}{q}\frac{dq'}{q'}F_i'(q,q') \times \left[\widehat{\mathsf{TS}}(q,p_t)+\frac{p_t}{q}D_i^\pi\left(\frac{p_t}{q}\right)\right]\cdot\left[\widehat{\mathsf{TS}}(q',p_b)+\frac{p_b}{q'}D_{i'}^\pi\left(\frac{p_b}{q'}\right)\right], \quad (10)$$

where $\widehat{\mathsf{TS}}$ represents TS recombination and $zD(z)$ represents fragmentation, which is identical to SS recombination. They are all known from previous studies [2, 4].

For fixed p_t and p_b it is possible to calculate the average fraction of energy loss by the away-side parton. One finds in central collision (c = 0.05) that for $p_t \sim 6$ GeV/c and $p_b \sim 4$ GeV/c [3]

$$\mathsf{f}_{\text{away}} \equiv \left\langle \frac{k'-q'}{k'} \right\rangle_{p_t,p_b} \approx 0.8 \quad . \quad (11)$$

That is to be compared to the near-side energy loss

$$\mathsf{f}_{\text{near}} \equiv \left\langle \frac{k-q}{k} \right\rangle_{p_t} \approx 0.15 \quad (12)$$

for $p_t \sim 6$ GeV/c. This large difference signifies the important properties of jet production in heavy-ion collisions in that there is trigger bias on the near side and anti-trigger bias on the away side. That is, when a trigger particle is used to select a subset of events, the hard-scattering point is biased toward being close to the near side to favor the production of a hadron in the presence of substantial momentum degradation in the dense medium. The selected events have on average lower f_{near} compared to random events. Shorter path length on the near side means longer path length on the away side, resulting in larger energy loss, hence larger f_{away}. For $c = 0.05$ and $p_T > 4$ GeV/c the average DPL $\langle\beta t\rangle$ is around 0.19, small compared to the average dynamical thickness βL of the medium, 2.9. Thus the thickness of the layer near the surface when hard partons are created is roughly $2\langle t\rangle/L \sim 0.13$ of L. The anti-trigger bias means that if a hadron at p_b is demanded on the away side within the subset of events triggered by a given p_t, then the average parton momentum $\langle k'\rangle_{p_t,p_b}$ must be much larger than $\langle k\rangle_{p_t}$ in order for the recoil parton to survive the medium effect to produce the away-side hadron at p_b.

For the yield at various centralities c, it is necessary to first include the c dependencies in the thermal distribution $T(q)$ and the hard parton distribution $f_i(k)$ and then to perform the averages over ξ using $P(\xi,c)$, i.e., we have for single-pion distribution

$$\frac{dN_\pi(c)}{p_t dp_t} = \int d\xi P(\xi,c)\frac{dN_\pi(c,\xi)}{p_t dp_t}, \quad (13)$$

and for two-pion distribution

$$\frac{dN_{\pi\pi}(c)}{p_t p_b dp_t dp_b} = \int d\xi P(\xi, c) \frac{dN_{\pi\pi}(c, \xi)}{p_t p_b dp_t dp_b}. \tag{14}$$

The per-trigger yield on the away-side is then

$$Y_{\pi\pi}^{\rm away}(p_t, p_b, c) = \frac{dN_{\pi\pi}(c)}{p_t p_b dp_t dp_b} \Bigg/ \frac{dN_\pi(c)}{p_t dp_t} \, . \tag{15}$$

Similar equation can be written for the near-side yield $Y_{\pi\pi}^{\rm near}(p_t, p_a, c)$. There are no adjustable parameters in the calculation. Fig. 4 shows the result for $Y_{\pi\pi}^{\rm near}(p_t, p_a, c)$ as functions of c for $p_t = 4$ and 6 GeV/c. The solid lines represent the integrated yield for $2 < p_a < 4$ GeV/c, the upper one for $p_t = 6$ GeV/c and the lower one for $p_t = 4$ GeV/c. The latter agrees well with the data available for $3 < p_t < 4$ GeV/c and $p_a > 2$ GeV/c [6]. The result shows very little dependence on c. That is reasonable because the hard-scattering point is close to the near-side surface, so the yield is insensitive to how large the main body of the medium is on the away side.

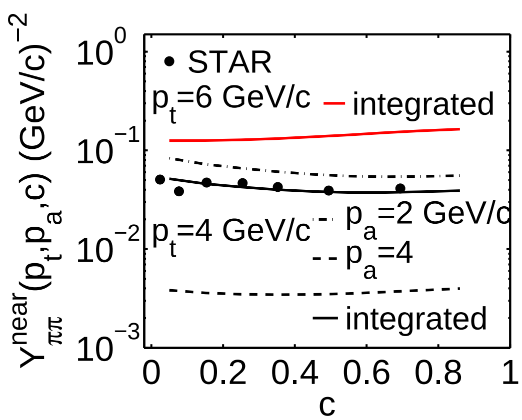

Figure 4: (Color online) Yield per trigger in the near-side jet as functions of centrality c for $p_t = 4$ GeV/c in black lines and $p_t = 6$ GeV/c in red line. Dash-dotted line is for $p_a = 2$ GeV/c and dashed line for $p_a = 4$ GeV/c. The solid lines are for the yields integrated over p_a from 2 to 4 GeV/c. The data are from Ref. [6].

To compare the near-side and away-side yields, we show them in Fig. 5(a) and (b) for fixed $c = 0.05$ and 0.35 and for $p_t = 4, 6, 8$ GeV/c, plotted against p_a and p_b. Note first that $Y_{\pi\pi}^{\rm away}$ is relatively insensitive to p_t compared to $Y_{\pi\pi}^{\rm near}$, an aspect of the anti-trigger bias versus trigger bias. The dependence on c is reversed, i.e. $Y_{\pi\pi}^{\rm near}$ is roughly independent of c as noted in the previous paragraph, but $Y_{\pi\pi}^{\rm away}$ increases by a factor of about 2 when c is raised from 0.05 to 0.35. The reason is that when the nuclear overlap is smaller, it is easier for the recoil jet to reach the away side and to produce a pion at p_b. With careful attention paid to the vertical scales of the two panels in Fig. 5, one sees that $Y_{\pi\pi}^{\rm away}$ is about an order of magnitude lower than $Y_{\pi\pi}^{\rm near}$. That is clearly a manifestation of the hard-scattering point being closer to the near side so that near-side jet suffers less energy loss than the away-side jet. The qualitative notions that form the conventional wisdom are now quantified by concrete calculations.

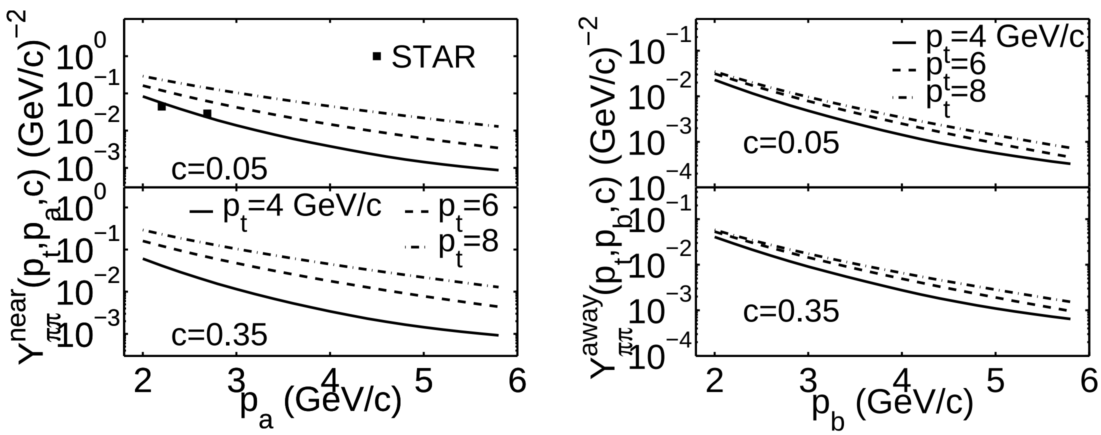

Figure 5: (a) Yield per trigger in the near-side jet as functions of p_a for two values of c and three values of p_t. (b) Yield per trigger in the away-side jet plotted in the same format as in (a) with p_a replaced by p_b.

4 Symmetric Dijets

Since the hard-scattering point is near the trigger side, we do not get a controlled look at the dense medium in the middle. One way to ensure that the hard-scattering point is midway between the two exit points is to consider symmetric dijets for which $p_t = p_b$. If we denote the common momentum by p ($= p_t = p_b$), we can calculate $\langle q' \rangle_p$ and $\langle k' \rangle_p$ separately for each c and show their ratio vs p, as in Fig. 6(a). The dependence on c is very mild; the value of $\langle q' \rangle / \langle k' \rangle$ is approximately 0.8 for all p shown. This result is very different from what one would obtain if βL is fixed at 2.9, for which $\langle q' \rangle / \langle k' \rangle \approx 0.24$ [3]. This three-fold increase is due to holding c fixed, instead of the DPL. The interpretation is that, since $\langle q' \rangle / \langle k' \rangle$ is a measure of the momentum survivability on the away side (which is the same as on the near side due to the symmetry imposed by $p_t = p_b$), there is much less energy loss on both sides at fixed c than at fixed medium thickness. Returning to Fig. 2(b) one sees that for every value of c there is wide variation of the DPL ξ. At $c = 0.05$ (not shown), one has

$\bar{\xi}(c) = \beta L = 2.9$, but ξ can still be very small for tangential trajectories, for which the momentum degradation is low and the survivability of the parton is high. Hadron production with $p_t = p_b > 3$ GeV/c favors events with large parton momentum $q \approx q'$, which in turn favors short DPL ξ. That is difficult for fixed $\beta L = 2.9$, but easy for fixed c, which is the experimental reality. Thus the implication of the result shown in Fig. 6(a) is that symmetric dijets are dominated by tangential jets.

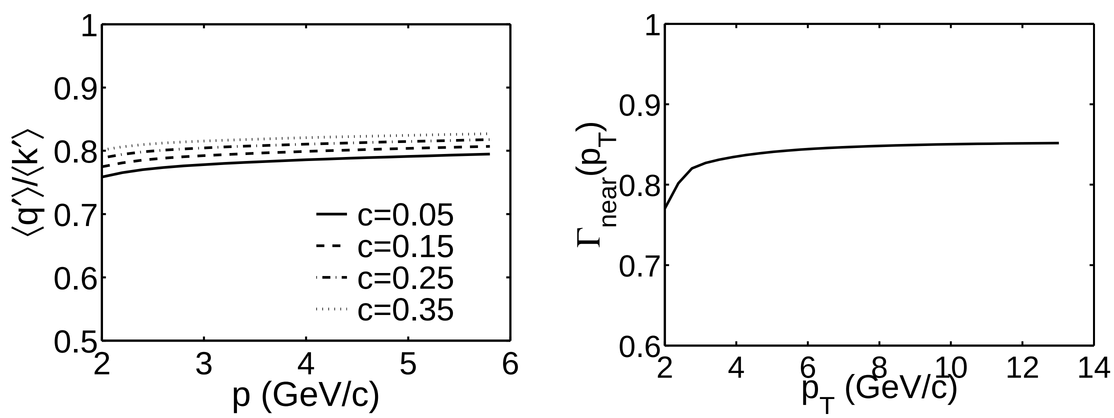

Figure 6: (a) The ratio $\langle q' \rangle / \langle k' \rangle$ at the symmetry point $p = p_t = p_b$ for four values of centrality. (b) Near-side survivability factor at $\beta L = 2.9$ as function of pion momentum p_T.

An independent check of the above result is to compare $\langle q' \rangle / \langle k' \rangle$, which involves averages over q' and k' in the two-particle distribution at the symmetry point, with $\langle q/k \rangle$ studied in [3], where the average is taken over q and k in the single-particle distribution for fixed $\beta L = 2.9$. That average ratio $\langle q/k \rangle$ is denoted by $\Gamma_{\rm near}$, representing the near-side survivability factor, and is shown in Fig. 6(b). $\Gamma_{\rm near} = 1$ means no momentum degradation. It is evident that panels (a) and (b) are similar in magnitude and shape for comparable ranges of p or p_T, yet $\Gamma_{\rm near}$ contains no information about the away-side jet. We already know that for fixed βL the hard-scattering point is near the surface and the hard parton loses only 15% of its momentum. Combining Fig. 6(a) and (b) leads to the conclusion that for symmetric jets both partons going in opposite directions lose the same fraction of momentum as if both are near the surface. To have both be near the surface can only mean that the jets are tangential within a thin layer for any centrality.

This is a remarkable result that emerges from theoretical considerations only. It has experimental support from the STAR data analyzed a year earlier on 2jet+1 correlation, which uses two opposite and nearly equal jets as trigger and studies the azimuthal distribution of the third associated particle [7]. Firstly no ridges are found, and secondly the yield depends on the number of participants as $N_{\rm part}^{2/3}$. Both features suggest that the two trigger jets are tangential. There is an elaborate story about the formation of ridges [8], the essence of which is that a ridge particle is the recombination product of enhanced thermal partons locally excited by the passage of a hard parton through the dense medium. Due to the flow of the thermal partons normal to the surface, there is a strong azimuthal correlation between a ridge particle and the jet [9]. A tangential jet is essentially defined by its direction being perpendicular to the vector normal to the surface at the nearest point. Such an orthogonal relationship is outside the width of azimuthal correlation (which is only 0.33), resulting in a strong suppression of the ridge formation. That is what is found in [7]. The $N_{\rm part}^{2/3}$ dependence is clearly a result of production near the surface, so it adds to the implication that the dijets are tangential. From our understanding of azimuthal correlation we can further conclude that the per-trigger yield of the particles associated with symmetric dijets should be relatively independent of centrality.

5 Conclusion

An exhaustive investigation of dihadron correlation at intermediate p_T has been carried out, only some of whose results are presented here. Near-side yield $Y_{\pi\pi}^{\rm near}(p_t, p_a, c)$ and away-side yield $Y_{\pi\pi}^{\rm away}(p_t, p_b, c)$ as functions of hadron momenta and centrality describe the properties of correlations that quantify the qualitative notion of trigger and anti-trigger biases. Averages of parton momenta at the points of creation in the medium and of emergence from the medium provide information about fractional energy loss. Such information leads to the realization that symmetric dijets are dominated by tangential jets, since hard partons created in the medium interior lose too much energy in getting out to be able to compete effectively with semihard partons created near the surface. That does not bode well for jet tomography. The problem is that at any centrality there are always short trajectories at some azimuthal angle.

The scenario described above is for measurable observables that average over all azimuthal angles ϕ. Recent results from analyses of RHIC data exhibit the ϕ dependencies of single-particle and correlation distributions [10, 11, 12]. In non-central collisions the ranges of possible path lengths can depend significantly on the ϕ angle, so more information on the nature of energy loss can be extracted from such data. While some progress has been made in understanding the ϕ dependence at low p_T [13], more work remains to be done for jet production at intermediate p_T, on which this paper represents only a beginning. Semihard scattering plays a major role in the ϕ dependence of the spectra at $2 < p_T < 6$ GeV/c, and therefore in $v_2(p_T, c)$ where thermal-shower recombination cannot be ignored [14]. To combine the azimuthal study of that work with the dijet study of this work should provide a very fruitful framework for probing the dense medium.

Acknowledgment

The work presented in this talk was done in collaboration with Chunbin Yang whose participation was essential. This work was supported, in part, by the U. S. Department of Energy under Grant No. DE-FG02-96ER40972

References

[1] S. S. Adler *et al.* (PHENIX Collaboration), Phys. Rev. C **76**, 034904 (2007).

[2] R. C. Hwa and C. B. Yang, Phys. Rev. C **70**, 024905 (2004).

[3] R. C. Hwa and C. B. Yang, Phys. Rev. C **79**, 044908 (2009).

[4] R. C. Hwa and C. B. Yang, Phys. Rev. C **70**, 024904 (2004); **73**, 064904 (2006).

[5] D. K. Srivastava, C. Gale, and R. J. Fries, Phys. Rev. C **67**, 034903 (2003).

[6] J. Putschke (for STAR Collaboration), Nucl. Phys. A **783**, 507c (2007).

[7] O. Barannikova, (for STAR Collaboration), talk given at Quark Matter 2008, Jaipur, India, J. Phys. G: Nucl. Part. Phys. **35**, 104086 (2008).

[8] R. C. Hwa, arXiv: 0904.2159, to be published in *Quark Gluon Plasma 4*, edited by R. C. Hwa and X. N. Wang (World Scientific, Singapore, 2009).

[9] C. B. Chiu and R. C. Hwa, Phys. Rev. C **79**, 034901 (2009).

[10] S. Afanasiev *et al.* (PHENIX Collaboration), arXiv: 0903.4886.

[11] A. Feng, (for STAR Collaboration), J. Phys. G: Nucl. Part. Phys. **35**, 104082 (2008).

[12] W. Holzmann, talk given at Quark Matter 2009; arXiv: 0907.4833.

[13] R. C. Hwa and L. L. Zhu, arXiv: 0909.1542.

[14] C. B. Chiu, R. C. Hwa, and C. B. Yang, Phys. Rev. C **78**, 044903 (2008).